

Showcasing research from Ewen Bodio and Christine Goze's group at ICMUB - Université de Bourgogne Franche-Comté, France.

In vitro and *in vivo* trackable titanocene-based complexes using optical imaging or SPECT

Two new gold(III)-BODIPY-imidazole based homobimetallic theranostics displaying both antiproliferative properties on different cancer cell lines and anti-inflammatory effect have been synthesized, characterized, and tracked *in vitro* at submicromolar range.

We warmly acknowledge Mr. Tangi Bodio for his help in the design of this cover artwork.

As featured in:



See Maria Paula Cabral Campello, Ewen Bodio, Pierre Le Gendre et al., *Dalton Trans.*, 2017, 46, 14548.

Cite this: *Dalton Trans.*, 2017, **46**, 14548

In vitro and *in vivo* trackable titanocene-based complexes using optical imaging or SPECT†

Océane Florès,^a Audrey Trommenschlager,^a Souheila Amor,^a Fernanda Marques,^b Francisco Silva,^b Lurdes Gano,^b Franck Denat,^a Maria Paula Cabral Campello,^b Christine Goze,^a Ewen Bodio^{*a} and Pierre Le Gendre^{*a}

A novel Ti/¹¹¹In-heterometallic radiotheranostic along with non-radioactive Ti/In, Ti/Lu, and Ti/Y analogues has been reported, thanks to the design of a challenging synthesis of the first titanocene-DOTA ligand. The corresponding titanocene-BODIPY complex was developed for *in vitro* tracking by optical imaging. The different complexes were characterized and their antiproliferative properties were evaluated on three cancer cell lines (A2780, B16F1, and PC3). As a proof of concept, initial studies in healthy mice were performed with a Ti/¹¹¹In derivative to obtain information about its uptake, its biodistribution, and its excretion. Confocal microscopy experiments were performed with fluorescent complexes to track it *in vitro*.

Received 1st June 2017,
Accepted 27th June 2017

DOI: 10.1039/c7dt01981e

rsc.li/dalton

Introduction

Among the numerous metals studied for their biological activities, most of them are electron rich metals, so-called “late metals” (e.g. platinum, ruthenium, gold, copper *etc.*), while electron poor metals – “early metals” – are much less studied.^{1,2} Nevertheless, titanium complexes appeared to be worth studying because of their anticancer properties.^{3–7} At the end of the 70s, Köpf and Köpf-Maier reported the first anticancer Ti-based complex: titanocene dichloride (Fig. 1).^{8,9} They based their choice on its structural analogy with cisplatin.¹⁰ Indeed, its two close chlorido ligands allow thinking that it can intercalate between DNA bases like cisplatin. Titanocene dichloride displayed promising results both *in vitro* and *in vivo*.^{11,12} Thus, it entered clinical trials in the early 90s as a novel potential anticancer agent.^{12,13} Unfortunately, it was dropped in phase II due to a lack of efficacy in patients.¹⁴ Among the cited reasons for this failure, its poor solubility and

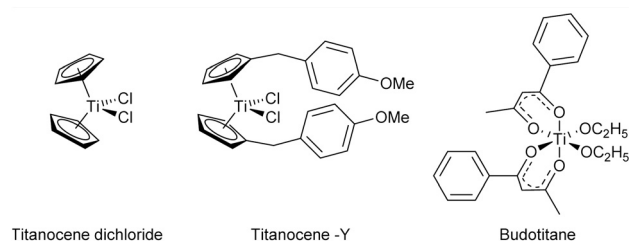


Fig. 1 Structures of three Ti-based complexes. Concerning budotitane, other isomers are possible.

stability in water appeared to be the major issue.^{15,16} As a result, during the last 30 years, numerous studies have reported the biological evaluation of differently substituted titanocenes (e.g. titanocene Y¹⁷),^{18–24} budotitane, which fail in clinical trials,^{25–27} or post titanocenes (e.g. Tshuva's complexes)^{6,28–30} for improving the efficacy of the complexes, their water solubility, and their resistance to hydrolysis (Fig. 1). An alternative strategy has been reported more recently: it consists of using nano-structured materials as safe vehicles for delivering titanocene complexes.³¹

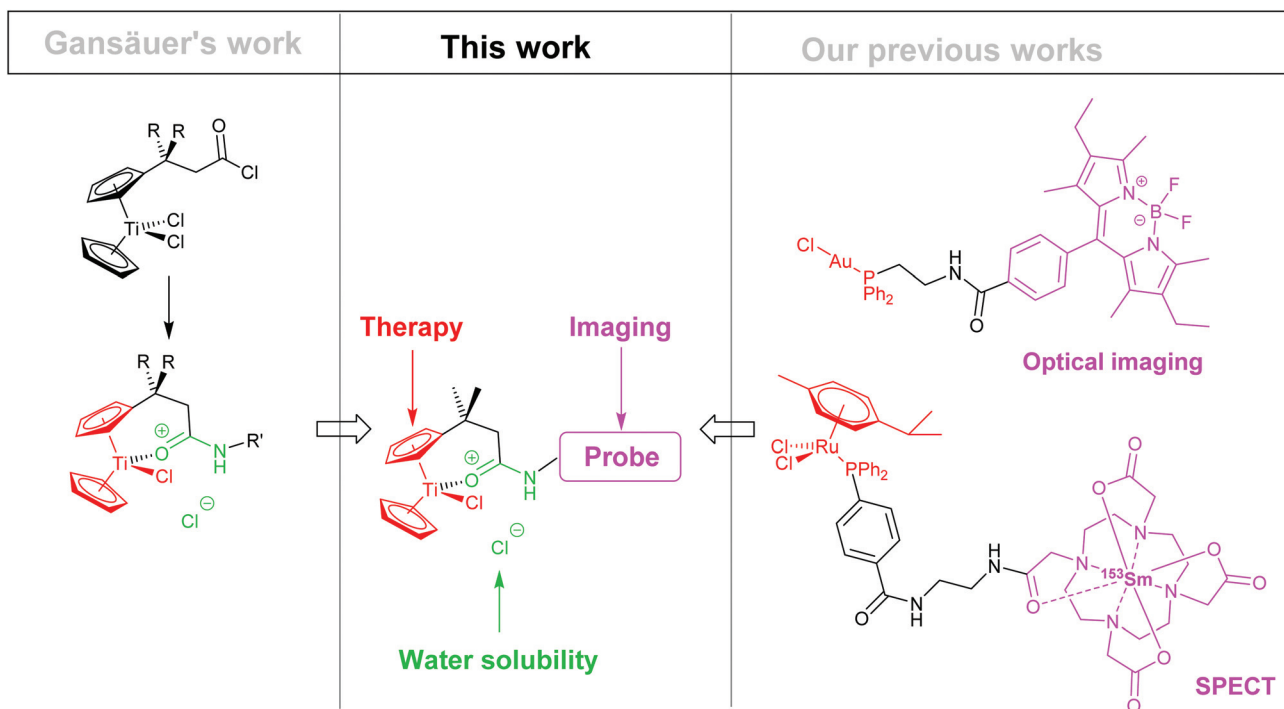
Another challenge faced by Ti-based complexes is the determination of their mechanism of action *in vitro* and *in vivo*. To date, contrary to the first hypothesis suggesting that titanocene dichloride behaves as cisplatin, at least “10 distinct mechanisms of action have been proposed for titanium-based therapeutics”.^{4,32,33} Cini, Bradshaw, and Woodward published a few months ago a very interesting tutorial review to deal with this subject.⁴

Such issues prompted us to design trackable Ti based therapeutics. Only a few trackable titanium complexes have been

^aICMUB UMR6302, CNRS, Univ. Bourgogne Franche-Comté, F-21000 Dijon, France. E-mail: ewen.bodio@u-bourgogne.fr, pierre.le-gendre@u-bourgogne.fr; Tel: +33 3 80 39 60 76

^bCentro de Ciências e Tecnologias Nucleares, Instituto Superior Técnico, Universidade de Lisboa, Estrada Nacional 10, Km 139.7, 2695-066 Bobadela LRS, Portugal. E-mail: pcampello@ctn.tecnico.ulisboa.pt

† Electronic supplementary information (ESI) available: Syntheses details, NMR spectra and data, HRMS data, HPLC chromatogram, stability studies, photo-physical data and spectra, radiolabelling details, and *in vitro* experimental data (antiproliferative tests, confocal imaging, live optical imaging movies, [¹¹¹In]-Ti-DOTA-In-1 uptake, and biodistribution studies in mice). See DOI: 10.1039/c7dt01981e



Scheme 1 Strategy envisioned in this work: combination of Gansäuer's synthesis of water soluble titanocene and our experience in grafting probes to metal complexes (only one configuration of titanium is represented in the scheme for the purpose of clarity but all the compounds are synthesized as racemic mixtures).

described to date. Some studies have reported the use of ⁴⁵Ti, which is a β⁺-emitter (3.1 h half-life), to perform PET (Positron Emission Tomography).^{34,35} These articles are really interesting but ⁴⁵Ti is poorly available and the strategy employed is limited to salan complexes or *in situ* generated transferrin Ti complexes and is not suitable for titanocene complexes.

Concerning *in vitro* tracking, surprisingly we did not find any *in vitro* study involving a fluorescent probe.† Dillon reported the use of X-ray fluorescence for mapping the distribution of Cp₂TiCl₂ in cells, but the study highlights the lack of sensitivity of this technique to obtain exploitable data.³⁶

Over the past few years, we have developed trackable complexes of late metals to gain insights into their mechanism of action.^{37–47} In the present work, we decided to apply the same strategy to early metal complexes and more precisely to titanocene complexes. We targeted titanocene complexes functionalised with a fluorescent probe, ideal for *in vitro* visualization of metal complexes, and complexes functionalised with a chelating agent for a radiometal, which is much more adapted for *in vivo* imaging (Scheme 1).

Concerning the fluorescent probe, BODIPY was selected, thanks to its high chemical stability and quantum yield, including in physiological media.^{48–50} For *in vivo* tracking, we selected a macrocycle (DOTA) to chelate radioactive metals for enabling SPECT (Single Photon Emission Computed Tomography) or PET studies. The synthesis of such titanocene

complexes is particularly challenging. One might envisage a conventional three step sequence consisting of the synthesis of probe-functionalised cyclopentadienyl ligands, deprotonation, and salt metathesis with a CpTiCl₃ precursor. However, undesired reactions between the probe and the base and/or with the highly oxophilic titanium precursor can be anticipated. To avoid these issues, we decided to draw our inspiration from Gansäuer's work (Scheme 1). Indeed, Gansäuer developed a clever strategy to functionalize *a posteriori* titanocene derivatives by developing a titanocene bearing a highly electrophilic acyl chloride. More than just making it possible to introduce different amines, this method results in the formation of cationic titanocenes.⁵¹ Very interestingly, despite moderate anti-proliferative properties, these complexes are water soluble and stable for several hours in physiological media (excepting a more or less rapid exchange of the chlorido ligand by a water molecule).

Thus, we decided to take advantage of this post functionalization to design water soluble trackable titanocene complexes and graft the probe in the final stage, which is highly advised when working with radionuclides.

Results and discussion

Synthesis

The titanocene carboxylate **1** was prepared according to Gansäuer's four step procedure and can be stored for several

† Gansäuer only suggests the possibility of using a pyrene for doing so.⁵⁶

months at room temperature even when air-packed.⁵¹ Complex **1** was then activated by thionylchloride to furnish acyl chloride **2**, which is directly reacted with the desired amine in the presence of sodium hydride (Scheme 2). One can notice that depending on the amine, the protocol needs to be carefully tuned: solvent, stoichiometry, reaction time, treatment *etc.* especially, we took advantage of the usual acidic treatment to hydrolyse the ester arms of the DOTA macrocycle **5** right after the coupling reaction with **2** to obtain a free carboxylic acid complex **Ti-DOTA-1**.

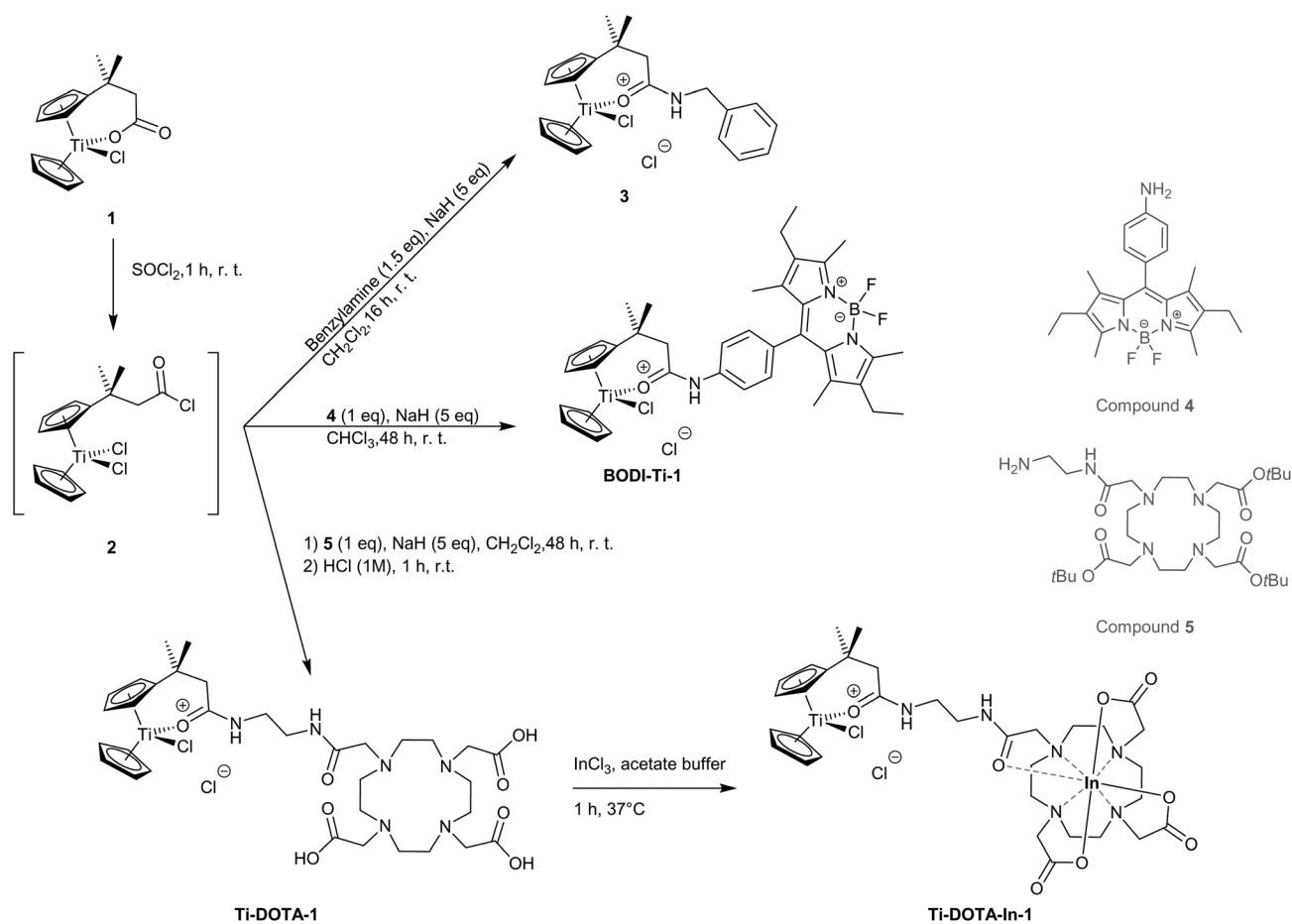
The synthesis of **Ti-DOTA-1** was particularly challenging due to the high oxophilicity of Ti(IV). To succeed, titanocene derivatives must not be used in the presence of a carboxylate, and therefore, we decided to use a DOTA precursor bearing protected ester arms, which can be hydrolysed thereafter. It may be the reason why, to the best of our knowledge, it is the first titanocene-polyazamacrocycle ever reported. It is worth noting that once the carbonyl is coordinated to titanium, the complex is far less sensitive to nucleophiles such as carboxylate groups or even water *etc.* This stability enables the purification of the complexes on preparative HPLC. Moreover, this strategy may be transposed to the preparation of cationic titanocenes bearing unprotected amino-acid (previously, only

“ester”-protected amino-acids have been tethered to titanocenes (Scheme 1)⁵¹). With **Ti-DOTA-1** in hand, a complexation study was performed on non-radioactive indium to optimize the reaction conditions for the subsequent radiometallation. The complexation of In(III) is quantitative after 1 h of reaction at 37 °C in acetate buffer (pH ≈ 5.7) (Scheme 2). Similar results have been obtained for Lu(III) and Y(III) (see the ESI† for details).

Photophysical characterization

The photophysical properties of the new fluorescent complex **BODI-Ti-1**, as well as the corresponding BODIPY-aniline **4**, were measured in DMSO (Table 1).

The two compounds present the classical absorption features of the BODIPY, *i.e.* an S₀-S₁ transition absorption band around 525 nm, and the S₀-S₂ absorption band around 380 nm (see the ESI† for details). The presence of “NH₂” in compound **4** induces a strong quenching of the fluorescence, which can be explained by a PET (Photoinduced Electron Transfer), while the formation of the amide link leads to the recovery of the fluorescence. It is worth noting that, contrary to some “late metals” (*e.g.* copper, platinum, ruthenium), the



Scheme 2 Synthesis of the different titanocene derivatives **3**, **BODI-Ti-1**, **Ti-DOTA-1**, and **Ti-DOTA-In-1** (only one configuration of titanium is represented in the scheme for the purpose of clarity but all the compounds are synthesized as racemic mixtures).

Table 1 Photophysical data of compounds **4** and **BODI-Ti-1** in DMSO at 293 K ($\lambda_{\text{exc}} = 488$ nm)

Compound	λ_{abs} (nm)	λ_{em} (nm)	ϵ ($\text{M}^{-1} \text{cm}^{-1}$)	Φ_f^a (%)
4	522	539	31 000	0.4
BODI-Ti-1	526	539	26 000	82

^a Rhodamine 6G ($\Phi_f = 92\%$, $\lambda_{\text{exc}} = 530$ nm, in water).⁵²

presence of titanium does not affect the fluorescence emission.

In vitro imaging

The localization of the complex **BODI-Ti-1** in cells was investigated by confocal microscopy (Leica TCS SP8). PC3 and B16F10 cells are incubated with a low concentration of **BODI-Ti-1** (1 μM) for 4 h at 37 °C. The significant intensity of fluorescence collected after 4 h of incubation confirms the excellent photophysical properties of **BODI-Ti-1** and indicates an excellent cell uptake of these complexes.

The resulting images clearly indicate an accumulation of **BODI-Ti-1** in the cytoplasm and not in the nucleus. At low concentrations, the distribution of the complex seems homogeneous in the cytoplasm (Fig. 2A). However, when **BODI-Ti-1** is imaged at 25 μM (and even more at 50 μM – data not

shown), a stronger fluorescence can be observed close to the nuclear membrane along with specific spots in the cytoplasm. Thus, **BODI-Ti-1** may preferentially accumulate in the mitochondria, in the endoplasmic reticulum, and/or in Golgi apparatus (Fig. 2B).

Evaluation of antiproliferative properties

The antiproliferative properties of the six Ti-based complexes (**3**, **BODI-Ti-1**, **Ti-DOTA-1**, **Ti-DOTA-In-1**, **Ti-DOTA-Lu-1**, and **Ti-DOTA-Y-1**) were evaluated on human ovarian (A2780), mouse melanoma (B16F1), and human prostate (PC3) cancer cell lines (see the ESI† for details). After 72 h of incubation, Gansäuer's complex **3** displays low cytotoxicity in the different cell lines (40–60% cellular viability at 200 μM), while the BODIPY derivative **BODI-Ti-1** displays strongly better antiproliferative properties (50–60% viability at 20 μM). DOTA derivatives do not display significant cytotoxicity even at 200 μM .

Gansäuer suggested that the differences he observed comparing the IC_{50} values of the complexes of his choice could be explained by the steric hindrance of Ti-based complexes or their ability to react with DNA. However, according to our results, the key parameter seems to be the cell uptake of the complexes. Indeed, an optical imaging study suggests a high uptake of **BODI-Ti-1** in cells (Fig. 2), while a cellular uptake study with a radioactive complex [¹¹¹In]-**Ti-DOTA-In-1** indicates a very low uptake (<1%) of the complex in A2780, B16F1, and PC3 even after 48 h of incubation (see the ESI† for details). In the present work, this uptake seems to be regulated by the hydrophilic/lipophilic balance of the complexes.

In future work, it would be interesting to graft a vector to Ti-DOTA derivatives for enabling the complexes to enter the cells (e.g. steroid,⁵³ estrogen receptor modulator,⁵⁴ cholesterol *etc.*⁵¹), and therefore to significantly improve their antiproliferative properties.

Radiolabelling study

Complexation of ¹¹¹In. Radiolabelling of **Ti-DOTA-1** was performed according to the protocol fine-tuned for the complexation of a non-radioactive indium salt: 1 h at 37 °C in ammonium acetate buffer. The radiolabeling procedure led to the formation of the desired compound with a radiochemical yield of $\approx 62\%$. The purification was performed by HPLC leading to the complex [¹¹¹In]-**Ti-DOTA-In-1** in 28% overall yield.

Stability studies. Stability studies have been performed in cell culture medium and human serum (see the ESI† for details). These experiments indicate that the compound [¹¹¹In]-**Ti-DOTA-In-1** is stable in cell culture medium until 24 h, but at 48 h the formation of another species was observed. The compound is less stable in the presence of human serum since after 1 h another peak begins to appear on the chromatogram. This new peak grows in intensity with time during incubation and at 48 h this new species becomes the majority. It is worth noting that HPLC-MS studies on non-radioactive analogues indicate that the second species should differ only by its “X-type” ligand. Indeed, the mass spectrum

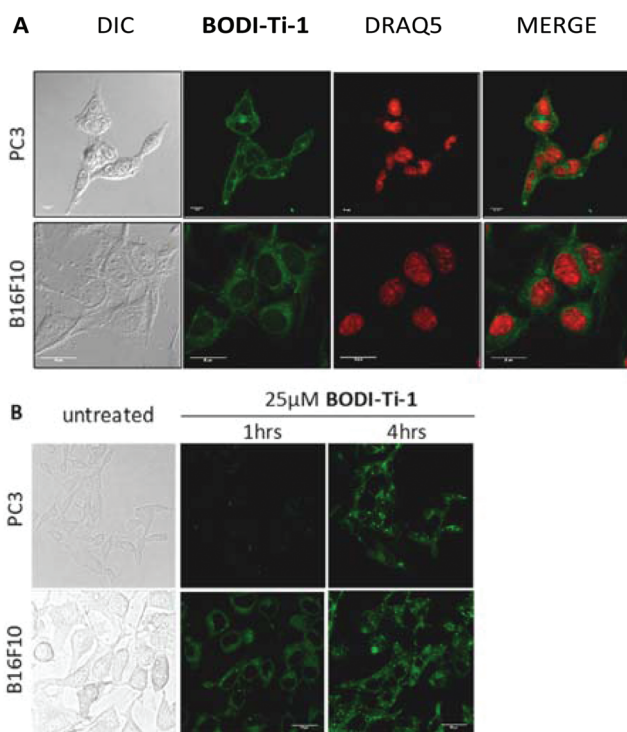


Fig. 2 Confocal immunofluorescence analysis of PC3 and B16F10 labelled with **BODI-Ti-1**. (A) Cells are incubated with 1 μM **BODI-Ti-1** (green) for 4 h at 37 °C and nuclei are counterstained with DRAQ5 (red, fluorescent DNA dye). (B) Cells are incubated with 25 μM **BODI-Ti-1** (green) for 1 h and 4 h at 37 °C in a H301 T Unit Bold Line top stage incubator (images were acquired during the time-lapse experiment).

obtained for the second peak indicates the dominance of the $[M - Cl]^{2+}$ ion. Thus, it is very likely that **Ti-DOTA-In-1** loses its chlorido ligand which is replaced by “-OH” or by a water molecule. As a consequence, the main structure of the bimetallic complex is stable and no release of ^{111}In was observed up to 48 h.

Preliminary *in vivo* study

To gain insight into the *in vivo* behaviour of the complex $[^{111}\text{In}]\text{-Ti-DOTA-In-1}$, preliminary tissue distribution studies were carried out in CD-1 mice. Data from these studies, expressed as % I.A. per g, at 15 min and 1 h p.i. are summarized for the most relevant organs in Fig. 3.

The biodistribution profile of the complex indicates a moderate blood clearance and a high kidney uptake (11.9 ± 5.0 and $11.0 \pm 2.2\%$ I.A. per g, at 15 min and 1 h p.i., respectively). No relevant radioactivity accumulation in any particular organ was found except for those highly vascularized like the liver, heart and lung. The kidney uptake associated with the overall excretion rate at these early time points (38.6 ± 4.2 and $59.5 \pm 4.7\%$ I.A., at 15 min and 1 h p.i., respectively) indicates the urinary tract as the predominant excretory pathway, which is in agreement with the strong hydrophilic character of the complex.

Experimental

General information

All of the analyses were performed at the “Plateforme d'Analyse Chimique et de Synthèse Moléculaire de l'Université de Bourgogne” (PACSMUB). The identity and purity of the compounds were unambiguously established using high-resolution mass spectrometry and NMR. High resolution mass spectra were recorded on a Thermo LTQ Orbitrap XL ESI-MS spectrometer. NMR spectra (^1H , ^{11}B , ^{19}F , ^{13}C) were recorded on Bruker 300 Avance III, 500 Avance III, or 600 Avance II spectrometers. Chemical shifts are given relative to TMS and were referenced to the residual solvent signal ^1H and ^{13}C . The list of abbreviations for signals in NMR is as follows: s = singlet, d =

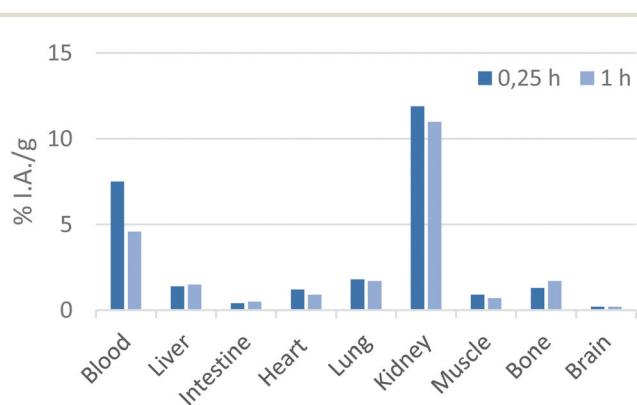


Fig. 3 Biodistribution of $[^{111}\text{In}]\text{-Ti-DOTA-In-1}$ at 15 min and 1 h after administration in CD-1 mice.

doublet, hept = heptuplet, m = multiplet, ps = pseudo-singlet, pt = pseudo-triplet, pq = pseudo-quadruplet and brs = broad singlet. Semi preparative HPLC were performed on a Thermo Scientific Dionex UltiMate 3000 system with an UltiMate 3000 diode array detector according to different methods which will be described thereafter. Analytical HPLC was performed using a Kinetex C18 2.6 μm -100 \AA , 2.1 \times 50 mm column with $\text{CH}_3\text{CN}/0.1\%$ TFA and $\text{H}_2\text{O}/0.1\%$ TFA eluents: linear gradient from 5% to 100% [$\text{CH}_3\text{CN}/0.1\%$ TFA] for 5 min, 100% [$\text{CH}_3\text{CN}/0.1\%$ TFA] for 2 min, returning to initial conditions by linear gradient for 0 to 95% [$\text{H}_2\text{O}/0.1\%$ TFA] for 1 min.

Synthesis

All reactions were carried out under an atmosphere of argon using standard Schlenk glassware or in a glove box, unless otherwise stated. All commercially available reagents were used without any further purification. CH_2Cl_2 and DMF were dried using an MBRAUN SPS 800 solvent purification system or distilled under argon from appropriate drying agents, and either used directly or stored under argon. DOTA derivative 5 was obtained from CheMatech®. Ti-Based complexes 1, 2, and 3 and BODIPY derivative 4 were synthesized following reported procedures.^{51,55}

BODI-Ti-1. In a Schlenk tube, titanocene-carboxylate 1 (40.6 mg, 0.130 mmol, 1 eq.) was dissolved in SOCl_2 (0.39 mL, 5.454 mmol, 42 eq.) and stirred for 1 h at room temperature. Excess SOCl_2 was removed under vacuum at 50 $^\circ\text{C}$ for 3 h. The resulting titanocene-acyl chloride was then dissolved in CHCl_3 (0.65 mL) and added to a mixture of NaH (15.6 mg, 0.649 mmol, 5 eq.) and BODIPY-aniline 4 (51.8 mg, 0.131 mmol, 1.01 eq.) in CHCl_3 (0.65 mL). The solution was stirred at room temperature for 48 h. After filtration by using a cannula, the resulting solution was evaporated and dried under vacuum, to obtain 5 as a red powder (54 mg, yield: 57%).

Ti-DOTA-1. In a Schlenk tube, titanocene-carboxylate 1 (102 mg, 0.326 mmol, 1 eq.) was dissolved in SOCl_2 (1 mL, 14 mmol, 42 eq.) and stirred for 1 h at room temperature. Excess SOCl_2 was removed under vacuum at 50 $^\circ\text{C}$ for 3 h. The resulting titanocene-acyl chloride 2 was then dissolved in CH_2Cl_2 (2 mL) and added to a mixture of NaH (39 mg, 1.630 mmol, 5 eq.) and DO3AtBu-N-(2-aminoethyl)ethanamide (201 mg, 0.326 mmol, 1 eq.) in CH_2Cl_2 (2 mL). The solution was stirred at room temperature for 48 h. After filtration through Celite, the resulting solution was washed with 1 M HCl (5 mL) and stirred for 1 h in order to hydrolyse the protecting ester arms. The aqueous layer was then isolated and evaporated to yield **Ti-DOTA-1** as a red powder (212 mg, crude yield = 84%).

Semi-preparative HPLC purification was performed on a BetaBasic C18, 5 μm , 30 \times 150 mm column using the following eluent system: 100% [$\text{H}_2\text{O}/0.1\%$ TFA] for 10 min, linear gradient from 0% to 40% [$\text{CH}_3\text{CN}/0.1\%$ TFA] for 40 min, 40% to 100% [$\text{CH}_3\text{CN}/0.1\%$ TFA] for 5 min, returning to initial conditions by linear gradient from 0 to 100% [$\text{H}_2\text{O}/0.1\%$ TFA] for 1 min. Purification yield = 30%.

Ti-DOTA-In-1. InCl₃ (6 mg, 0.0271 mmol, 1.05 eq.) is dissolved in 0.05 M HCl (4.5 mL). An aqueous solution of 1 M NH₄OAc (0.5 mL) is added to reach the desired pH value (≈ 5.7). **Ti-DOTA-1** (20 mg, 0.0257 mmol, 1 eq.) in 0.5 mL H₂O is then added and the mixture is stirred at 37 °C for 1 h. The solvent is then evaporated under vacuum.

Semi-preparative HPLC purification was performed on a BetaBasic C18, 5 μ m, 30 \times 150 mm column with the following eluent system: 100% [H₂O/0.1% TFA] for 15 min, linear gradient from 0% to 40% [CH₃CN/0.1% TFA] for 40 min, 40% to 100% [CH₃CN/0.1% TFA] for 5 min, returning to initial conditions by linear gradient from 0 to 100% [H₂O/0.1% TFA] for 1 min (14% ACN).

Ti-DOTA-In-1 is obtained as an orange powder (10 mg, 40%).

Photophysical measurements

UV-Visible absorption spectra were recorded on a JASCO V630BIO spectrometer. The steady-state fluorescence emission spectra were obtained by using a JASCO FP8500 spectrofluorometer instrument. All fluorescence spectra were corrected for instrument response. The fluorescence quantum yields (Φ_F) were calculated using the equation:

$$\frac{\Phi_F}{\Phi_{FR}} = \frac{n^2}{n_R^2} \times \frac{\int_0^\infty I_F(\lambda_E, \lambda_F) d\lambda_F}{\int_0^\infty I_{FR}(\lambda_E, \lambda_F) d\lambda_F} \times \frac{1 - 10^{-A_R(\lambda_E)}}{1 - 10^{-A(\lambda_E)}}$$

where Φ_F and Φ_{FR} are the fluorescence quantum yields of the compound and the reference respectively. $A(\lambda_E)$ and $A_R(\lambda_E)$ are the absorbances at the excitation wavelength, and n is the refractive index of the medium. I_F and I_{FR} are the fluorescence intensities of the compound and the reference respectively. Rhodamine 6G ($\Phi_F = 0.92$ in water) was used as the standard.⁵² In all Φ_F determinations, a correction for the solvent refractive index (n) was applied.

Photophysical data of the different compounds were determined in DMSO at 293 K.

Confocal microscopy experiments

Cells (PC3, B16F10) were seeded on a chambered coverglass (12 Well Chamber-ibidi) and allowed to recover. After 24 h, cells were incubated with 1 μ M of **BODI-Ti-1** for 4 h, and then washed with 1 \times PBS. For co-localization experiments, cells were fixed and permeabilized with iced methanol for 10 min at room temperature. Methanol was removed, the cells were incubated with a 5 μ M DRAQ5 solution for 5–10 min and then mounted with Fluoromount-G® (Southern Biotech).

Confocal imaging was performed using a confocal laser-scanning microscope (Leica TCS SP8) with a $\times 63$ HCX PL APO oil immersion (ON 1.4) objective lens, which allowed obtaining DIC (Differential Interference Contrast) and fluorescence images (1024 pixels \times 1024 pixels) simultaneously, and LASX software (Leica Microsystems, Ltd). The samples were excited using internal microscope lasers and the emission intensity was recorded at an appropriate emission wavelength. Fluorescence images were sequentially acquired. For co-localiz-

ation experiments, **BODI-Ti-1** (green) was excited at 488 nm and its emission was recorded from 493 to 600 nm, whereas DRAQ5 (red) was excited at 638 nm and its emission was recorded from 661 nm to 778 nm. Image processing and analyses were carried out using Fiji/ImageJ.

Cytotoxicity assays

The cell lines PC3 prostate, B16F1 melanoma (ATCC) and A2780 ovarian (Sigma-Aldrich) were cultured in RPMI 1640 (ovarian, prostate) or DMEM + GlutaMAX™-I (melanoma) medium supplemented with 10% fetal bovine serum (Gibco) at 37 °C, under a humidified atmosphere of 5% CO₂. All cells were adherent in monolayers and when confluent were sub-cultured with 0.05% trypsin-EDTA (Gibco) and splitted. The cytotoxicity of the compounds was evaluated by using the yellow tetrazolium salt MTT that is reduced by viable cells to yield purple formazan. For the cytotoxicity studies, cells (10^4 – 2×10^4 cells per well) were seeded in 96 well plates and incubated overnight. Stock solutions (20 mM) of the compounds were made in water or DMSO (**BODI-Ti-1**) and then diluted in a medium to the desired concentrations (0.1–200 μ M). For the higher concentration of the BODIPY compound in medium (50 μ M) the percentage of DMSO was 0.25%, which induced no cytotoxic effect. Cells were incubated with the compounds in media for 24 and 48 h. At the end of the incubation period, the compounds were removed and the cells were incubated with 0.2 mL of MTT solution (0.5 mg mL⁻¹ phosphate buffered saline (PBS)). After 3 h at 37 °C, 5% CO₂, the medium was removed and the purple formazan crystals were dissolved in 0.2 mL of DMSO by shaking. The cellular viability was evaluated by measuring the absorbance at 570 nm as previously described.³⁹ Each experiment was repeated at least twice and each concentration was tested in at least six replicates.

Radiolabeling procedure

40 μ L of ¹¹¹InCl₃ (700 μ Ci) were added to 200 μ L of InCl₃ (6 mg/4.5 mL, 0.05 M HCl). A CH₃COONH₄ solution (1 M, aq.) was added until reaching pH ≈ 5.5 (≈ 100 μ L) and then **Ti-DOTA-1** (22.5 μ L, 20 mg/500 μ L, aq.) was mixed. The solution was heated at 37 °C for 1 h.

The radiolabeling procedure leads to the formation of the desired compound [¹¹¹In]-**Ti-DOTA-1** with a radiochemical yield of $\approx 62\%$. After HPLC purification, the overall yield was $\approx 28\%$. CH₃CN and TFA of the HPLC solvents were removed using N₂. $t_r = 8.9$ min (method 1), $t_r = 6.4$ min (method 2).

HPLC method 1: Solvent A – TFA 0.1% (aq.), B – CH₃CN (0.1% TFA). 5% to 70% B for 15 min, 70% to 100% B for 1 min, 100% B for 4 min.

HPLC method 2: Solvent A – TFA 0.1% (aq.), B – CH₃CN (0.1% TFA). 5% to 100% B for 5 min, 100% B for 5 min.

Biodistribution

The *in vivo* behaviour of [¹¹¹In]-**Ti-DOTA-In-1** was evaluated in groups of 3 female CD-1 mice (randomly bred, Charles River, Spain) weighing approximately 25 g each. Animals were intravenously injected with 100 μ L (0.9–1.1 MBq) of the complex *via*

the tail vein and were maintained on normal diet *ad libitum*. At 15 minutes and 1 h post-injection (p.i.) mice were sacrificed by cervical dislocation. The radioactive dosage administered and the radioactivity in the sacrificed animals were measured using a dose calibrator (Capintec, CRC25R). The difference between the radioactivity in the injected and sacrificed animals was assumed to be due to excretion, mainly urinary excretion. Blood samples were collected by cardiac puncture at sacrifice. Tissue samples of the main organs were then removed, weighed and counted using a gamma counter (Berthold LB2111). The biodistribution results were expressed as the percent of injected activity per organ or g organ (% I.A. per g organ).

Conclusions

For the first time, one BODIPY-titanocene derivative and one DOTA-titanocene derivative were synthesized. Water soluble indium, lutetium, and yttrium heterometallic complexes were easily obtained starting from the corresponding free DOTA-titanocene. The same protocol has enabled obtaining a radioactive ^{111}In analogue and an *in vivo* preliminary biodistribution study proved the feasibility of tracking this complex by SPECT. Thanks to the first synthesis of a titanocene-BODIPY complex, it was established that such compounds can be efficiently tracked *in vitro* at low concentrations by optical imaging. Antiproliferative activity evaluation of the different complexes on several cancer cell lines highlights the importance of the complex cell uptake.

For future investigations on trackable titanocene therapeutics, it will be worthwhile to vectorise these complexes to increase their cell uptake, and therefore their therapeutic properties. To finish, we would like to add that it is important to keep in mind that the probe moiety will impact the biological properties of this kind of theranostic agent, thus, it has to be chosen and introduced into the molecule at the beginning of the study and prior to any optimization process.

Acknowledgements

Support was provided by the Conseil Régional de Bourgogne Franche-Comté (PARI II subprojects 2-p2 and 3-p2), the Ministère de l'Enseignement Supérieur et de la Recherche, the Centre National de la Recherche Scientifique (CNRS), and the French Research National Agency (ANR) *via* the project JCJC "SPID" ANR-16-CE07-0020. COST Actions TD1004 and FrenchBIC are acknowledged for fruitful discussion. DOTA derivative **5** was kindly provided by the company CheMatech®. Pr. Anthony Romieu and Dr V. Goncalves are acknowledged for fruitful discussion on HPLC, Dr Y. Volkova and Dr M. Ipuay for the synthesis of compound **4** precursor, and Ms J. Pineau for her help in the synthesis of complex **3**. Plateforme DimaCell, INRA, U. Bourgogne Franche-Comté, and F21000 Dijon, France

are acknowledged. C2TN/IST authors gratefully acknowledge FCT support through the UID/Multi/04349/2013 project.

Notes and references

- G. Gasser, I. Ott and N. Metzler-Nolte, *J. Med. Chem.*, 2011, **54**, 3–25.
- C. G. Hartinger and P. J. Dyson, *Chem. Soc. Rev.*, 2009, **38**, 391–401.
- K. M. Buettner and A. M. Valentine, *Chem. Rev.*, 2012, **112**, 1863–1881.
- M. Cini, T. D. Bradshaw and S. Woodward, *Chem. Soc. Rev.*, 2017, **46**, 1040–1051.
- Y. Ellahioui, S. Prashar and S. Gómez-Ruiz, *Inorganics*, 2017, **5**, 4.
- E. Y. Tshuva and J. A. Ashenhurst, *Eur. J. Inorg. Chem.*, 2009, **2009**, 2203–2218.
- K. Strohfeldt and M. Tacke, *Chem. Soc. Rev.*, 2008, **37**, 1174.
- H. Köpf and P. Köpf-Maier, *Angew. Chem., Int. Ed. Engl.*, 1979, **91**, 509–509.
- P. Köpf-Maier and H. Köpf, *Naturwissenschaften*, 1980, **67**, 415–416.
- G. Gasser, I. Ott and N. Metzler-Nolte, *J. Med. Chem.*, 2011, **54**, 3–25.
- P. Köpf-Maier, B. Hesse and H. Köpf, *J. Cancer Res. Clin. Oncol.*, 1980, **96**, 43–51.
- A. Korfel, M. E. Scheulen, H. J. Schmoll, O. Gründel, A. Harstrick, M. Knoche, L. M. Fels, M. Skorzec, F. Bach, J. Baumgart, G. Sass, S. Seeber, E. Thiel and W. E. Berdel, *Clin. Cancer Res.*, 1998, **4**, 2701–2708.
- C. V. Christodoulou, D. R. Ferry, D. W. Fyfe, A. Young, J. Doran, T. M. Sheehan, A. Eliopoulos, K. Hale, J. Baumgart, G. Sass and D. J. Kerr, *J. Clin. Oncol.*, 1998, **16**, 2761–2769.
- G. Lümmer, H. Sperling, H. Luboldt, T. Otto and H. Rübber, *Cancer Chemother. Pharmacol.*, 1998, **42**, 415–417.
- J. H. Toney and T. J. Marks, *J. Am. Chem. Soc.*, 1985, **107**, 947–953.
- J. H. Murray and M. M. Harding, *J. Med. Chem.*, 1994, **37**, 1936–1941.
- J. Claffey, M. Hogan, H. Müller-Bunz, C. Pampillón and M. Tacke, *ChemMedChem*, 2008, **3**, 729–731.
- N. J. Sweeney, O. Mendoza, H. Müller-Bunz, C. Pampillón, F.-J. K. Rehmann, K. Strohfeldt and M. Tacke, *J. Organomet. Chem.*, 2005, **690**, 4537–4544.
- T. Hodík, M. Lamač, L. Červenková Št'astná, J. Karban, L. Koubková, R. Hrstka, I. Císařová and J. Pinkas, *Organometallics*, 2014, **33**, 2059–2070.
- J. Ceballos-Torres, S. Prashar, M. Fajardo, A. Chicca, J. Gertsch, A. B. Pinar and S. Gómez-Ruiz, *Organometallics*, 2015, **34**, 2522–2532.
- C. Pampillón, J. Claffey, K. Strohfeldt and M. Tacke, *Eur. J. Med. Chem.*, 2008, **43**, 122–128.

- 22 O. R. Allen, L. Croll, A. L. Gott, R. J. Knox and P. C. McGowan, *Organometallics*, 2004, **23**, 288–292.
- 23 O. R. Allen, A. L. Gott, J. A. Hartley, J. M. Hartley, R. J. Knox and P. C. McGowan, *Dalton Trans.*, 2007, 5082.
- 24 P. W. Causey, M. C. Baird and S. P. C. Cole, *Organometallics*, 2004, **23**, 4486–4494.
- 25 H. J. Keller, B. Keppler and D. Schmähl, *J. Cancer Res. Clin. Oncol.*, 1983, **105**, 109–110.
- 26 B. K. Keppler, C. Friesen, H. G. Moritz, H. Vongerichten and E. Vogel, in *Bioinorganic Chemistry*, Springer, Berlin, Heidelberg, 1991, vol. 78, pp. 97–127.
- 27 P. Köpf-Maier, *Eur. J. Clin. Pharmacol.*, 1994, **47**, 1–16.
- 28 A. Tzuberly and E. Y. Tshuva, *Inorg. Chem.*, 2011, **50**, 7946–7948.
- 29 A. Tzuberly and E. Y. Tshuva, *Inorg. Chem.*, 2012, **51**, 1796–1804.
- 30 H. Glasner and E. Y. Tshuva, *J. Am. Chem. Soc.*, 2011, **133**, 16812–16814.
- 31 W. A. Wani, S. Prashar, S. Shreaz and S. Gómez-Ruiz, *Coord. Chem. Rev.*, 2016, **312**, 67–98.
- 32 J. Schur, C. M. Manna, A. Deally, R. W. Köster, M. Tacke, E. Y. Tshuva and I. Ott, *Chem. Commun.*, 2013, **49**, 4785–4787.
- 33 S. Gómez-Ruiz, D. Maksimović-Ivanić, S. Mijatović and G. N. Kaluderović, *Bioinorg. Chem. Appl.*, 2012, **2012**, e140284.
- 34 G. W. Severin, C. H. Nielsen, A. I. Jensen, J. Fonslet, A. Kjær and F. Zhuravlev, *J. Med. Chem.*, 2015, **58**, 7591–7595.
- 35 A. L. Vavere and M. J. Welch, *J. Nucl. Med.*, 2005, **46**, 683–690.
- 36 J. B. Waern, H. H. Harris, B. Lai, Z. Cai, M. M. Harding and C. T. Dillon, *JBIC, J. Biol. Inorg. Chem.*, 2005, **10**, 443–452.
- 37 B. Bertrand, P.-E. Doullain, C. Goze and E. Bodio, *Dalton Trans.*, 2016, **45**, 13005–13011.
- 38 E. Bodio, P. Le Gendre, F. Denat and C. Goze, *Adv. Inorg. Chem.*, 2016, **68**, 253–299.
- 39 L. Adriaenssens, Q. Liu, F. Chaux-Picquet, S. Tasan, M. Picquet, F. Denat, P. Le Gendre, F. Marques, C. Fernandes, F. Mendes, L. Gano, M. P. C. Campello and E. Bodio, *ChemMedChem*, 2014, **9**, 1567–1573.
- 40 M. Ali, L. Dondaine, A. Adolle, C. Sampaio, F. Chotard, P. Richard, F. Denat, A. Bettaieb, P. Le Gendre, V. Laurens, C. Goze, C. Paul and E. Bodio, *J. Med. Chem.*, 2015, **58**, 4521–4528.
- 41 P.-E. Doullain, S. Tasan, R. Decreau, C. Paul, P. Le Gendre, F. Denat, C. Goze and E. Bodio, *J. Biol. Inorg. Chem.*, 2014, **19**, S793–S793.
- 42 S. Tasan, O. Zava, B. Bertrand, C. Bernhard, C. Goze, M. Picquet, P. Le Gendre, P. Harvey, F. Denat, A. Casini and E. Bodio, *Dalton Trans.*, 2013, **42**, 6102–6109.
- 43 L. Dondaine, D. Escudero, M. Ali, P. Richard, F. Denat, A. Bettaieb, P. Le Gendre, C. Paul, D. Jacquemin, C. Goze and E. Bodio, *Eur. J. Inorg. Chem.*, 2016, **2016**, 545–553.
- 44 B. Bertrand, A. de Almeida, E. P. M. van der Burgt, M. Picquet, A. Citta, A. Folda, M. P. Rigobello, P. Le Gendre, E. Bodio and A. Casini, *Eur. J. Inorg. Chem.*, 2014, **2014**, 4410–4410.
- 45 P. D. Harvey, S. Tasan, C. P. Gros, C. H. Devillers, P. Richard, P. L. Gendre and E. Bodio, *Organometallics*, 2015, **34**, 1218–1227.
- 46 S. Tasan, C. Licon, P.-E. Doullain, C. Michelin, C. P. Gros, P. Le Gendre, P. D. Harvey, C. Paul, C. Gaiddon and E. Bodio, *JBIC, J. Biol. Inorg. Chem.*, 2014, **20**, 143–154.
- 47 A. Trommenschlager, F. Chotard, B. Bertrand, S. Amor, L. Dondaine, M. Picquet, P. Richard, A. Bettaieb, P. Le Gendre, C. Paul, C. Goze and E. Bodio, *Dalton Trans.*, 2017, **46**, 8051–8056.
- 48 J. Bañuelos, *Chem. Rec.*, 2016, **16**, 335–348.
- 49 G. Ulrich, R. Ziesel and A. Harriman, *Angew. Chem., Int. Ed.*, 2008, **47**, 1184–1201.
- 50 A. Loudet and K. Burgess, *Chem. Rev.*, 2007, **107**, 4891–4932.
- 51 A. Gansäuer, D. Franke, T. Lauterbach and M. Nieger, *J. Am. Chem. Soc.*, 2005, **127**, 11622–11623.
- 52 A. M. Brouwer, *Pure Appl. Chem.*, 2011, **83**, 2213–2228.
- 53 L. M. Gao, J. L. Vera, J. Matta and E. Meléndez, *JBIC, J. Biol. Inorg. Chem.*, 2010, **15**, 851–859.
- 54 S. Top, E. Kaloun, A. Vessières, I. Laïos, G. Leclercq and G. Jaouen, *J. Organomet. Chem.*, 2002, **643–644**, 350–356.
- 55 V. A. Azov, F. Diederich, Y. Lill and B. Hecht, *Helv. Chim. Acta*, 2003, **86**, 2149–2155.
- 56 A. Gansäuer, I. Winkler, D. Worgull, T. Lauterbach, D. Franke, A. Selig, L. Wagner and A. Prokop, *Chem. – Eur. J.*, 2008, **14**, 4160–4163.